Biomass volatiles reforming by integrated pyrolysis and plasma-catalysis system for H_2 production: Understanding roles of temperature and catalyst

Zhicheng Xu[a], Ningbo Gao[a, *], Yan Ma[a], Weitao Wang[b], Cui Quan[a], Xin Tu[b], Norbert Miskolczi[c]

[a] Xi'an Key Laboratory of Solid Waste Recycling and Resource Recovery, School of Energy and Power Engineering, Xi'an Jiaotong University, Xi'an, 710049, China

[b] Department of Electrical Engineering and Electronics, University of Liverpool, Liverpool, L69 3GJ, UK

[c] Faculty of Engineering, MOL Department of Hydrocarbon and Coal Processing, Institute of Chemical Engineering and Process Engineering, University of Pannonia, Veszprém, Hungary

nbogao@xjtu.edu.cn (corresponding author)

Abstract: Biomass utilization is considered a carbon-neutral way to simultaneously tackle the energy crisis and environmental contamination. Challenges still exist to hinder its application, such as low products yield, tar blockage, harsh condition and inferior stability. This paper aims to study whether the newly developed integrated pyrolysis and plasma-catalysis system can be applied into practice of H_2 production from real biomass volatiles, and to understand roles of temperature and catalyst. The experiments were performed in a two-stage reactor embedded with a coaxial dielectric barrier discharge plasma zone. Impacts of operating conditions (i.e. discharge power, steam input, heat supply and catalyst packing) on H_2 production were investigated. The results show that proper input of discharge power and steam can promote H_2 production. Heating supply is recognized as two different effects on plasma-only and plasma-catalysis systems, since reaction temperature elevation acts as inhibitor to plasma characters and cut down the contribution of plasma reforming. After packing bimetallic Ni-Fe/γ-Al_2O_3 catalyst into plasma, optimal 47.65 mmol/g of H_2 can be attained at reforming temperature of 500℃, with synergy effects observed. Plasma-catalysis system also outperformed in tar cracking, tar elimination and stability test, attributed to

plasma assistance. This work provides an alternative to construct a new plasma-catalysis process for H_2 production from biomass volatiles or to couple plasma technology with existing biomass conversion industries for preferable energy and fuel production, highlighting its promising commercialization prospects.

Keywords: Non-thermal plasma, biomass utilization, plasma-catalysis reforming, hydrogen production, catalyst stability

1. Introduction

How to tackle the energy crisis and environmental contamination has been a major concern hindering social development. Not only can using exhaustible fossil fuels threaten global energy security, but the emission of greenhouse gases will exacerbate climate change and ecological environment damage[1-3]. As a promising sustainable energy, biomass has come into public view owing to its broad sources, which furnishes around 15% energy consumption worldwide[4]. Appropriate utilization of biomass energy can achieve a carbon-neutral process or even a carbon sink, thanks to its ability to capture carbon dioxide from atmosphere during growth[5, 6]. Various technological means have been applied to biomass utilization for energy and valued material production such as, direct combustion[7], gasification[8], liquefaction[9], carbonization[10] and fermentation[11], etc. Hydrogen is perceived as an ideal next-generation energy carrier because of its high energy capacity and pollution-free utilization pathways[12-14]. A series of chemicals for example, methanol, ethanol and dimethylether (DME), etc., can be produced by using hydrogen as raw feedstock[15-17]. Therefore, hydrogen production from biomass pyrolysis/gasification can be deemed as a potential solution from both energy production and environmental

protection points of view.

Extensive researches have been devoted into the field of biomass pyrolysis/gasification in terms of feedstocks, facilities, operation parameters, conversion processes and products distribution, etc[18-20]. For purpose of its commercial development, tar contamination and high energy consumption are two major target problems to be settled. It is reported that tar with complex heavy hydrocarbons can vary in concentration from 1 g/Nm^3 to 100 g/Nm^3, which could clog downstream equipment[21]. Thereby, coupling biomass pyrolysis and catalytic steam reforming was developed to promote the products quality, where the attendant problems lie in the catalysts selection and performance optimization[22]. Instead of noble metals, nickel-based catalysts are highly favored in the processes of pyrolysis and reforming of biomass, due to its low cost and decent catalytic performance[23]. For example, Yao et al. achieved H_2 production from biomass using a two-stage fixed bed reactor coupling pyrolysis-gasification process with Ni-biochar catalyst at 900°C[24]. Whereas, relatively high temperature is of great necessity to ensure favorable catalytic performance, resulting in high energy demand and catalyst sintering. Bimetallic catalysts were turned out to be an effective approach for catalytic performance enhancement, among which Ni-Fe is believed to be profitable in tar reforming[25, 26]. Besides, sever coke deposition could lead to rapid catalyst deactivation and following system termination, which restrict the stabilization and application.

Great interests have been attached into non-thermal plasma (NTP) technology, which could allow occurrence of thermodynamically unfavorable reactions even at atmospheric pressure and temperature[27-30]. Highly energetic electrons with 1-10 eV electron energy can be generated, while a macroscopically mild reaction conditions can be maintained meanwhile[31, 32]. Energy can be transferred to reactants by collision,

leading to avalanche generation of various active species such as free radicals, excited atoms, ions and molecules, for follow-up reactions. Therefore, NTPs have been broadly applied to CO_2 conversion[33], ammonia synthesis[16], hydrocarbons cracking as well as tar reforming[34], etc. However, prominent problems were noticed in its low conversion efficiency and products selectivity, which could be properly solved by combining heterogenous catalyst with NTPs to make use of their synergy effects[35]. Dielectric barrier discharge (DBD) is commonly considered the most suitable NTP reactors to couple with catalyst, which possesses advantages in its simplicity, scalability as well as easy packing and collection of catalysts to ensure valid collaboration between plasma and catalysts[36-38]. Currently, there have been some works regarding plasma and catalyst for tar reforming processes, in terms of catalysts pretreatment by plasma, post-plasma-catalysis and in-plasma-catalysis reforming[39-41]. Nevertheless, tar model compounds including benzene, toluene and naphthalene were usually used for targets[42, 43]. Researches were rarely reported in aspects of volatiles derived from real complex biomass or combining biomass thermal conversion with plasma-catalysis technology, which may present totally dissimilar effectiveness with simulated compounds. Besides, tail gases out from biomass gasifier are always with high temperature, and operating conditions has crucial influence on catalysis and plasma performance, where scarce knowledge can be obtained for reference to date. Therefore, a comprehensive study is of great significance to understand the role of temperature and catalyst on plasma-catalysis process for biomass volatiles reforming, achieving superior performance of energy production from real biomass and further practical application.

This work aims to achieve an optimized H_2 production pathway from complex biomass pyrolysis/gasification volatiles, and to investigate influential factors of system,

providing reference for technology commercialization in fields of biomass utilization and plasma-based energy conversion. Herein, a novel integrated pyrolysis and plasma-catalysis system was developed to realize compact processes with subsequent biomass pyrolysis and plasma-catalysis reforming of volatiles for H_2 production. To understand roles of temperature and catalyst, different operating parameters including discharge power, steam input and heat addition, etc., were investigated to find optimal conditions, with packing γ-Al_2O_3 supported Ni-Fe bimetallic catalyst into plasma zone. The ability of tar removal from biomass volatiles and stability of system were also studied with performance experiments and characterizations to demonstrate the synergy effects between catalyst and plasma. Further, the proposed mechanisms were elaborated to highlight promising superiorities and application prospects of this novel system in H_2 production from complex biomass volatiles.

2. Materials and methods

2.1 Materials

As a kind of extensively used and representative biomass, pine sawdust was selected as the biomass feedstock for hybrid pyrolysis and plasma catalysis system in this study. The pine sawdust feedstock was processed with an electric shaker to sieve to particle size of 60 mesh. The proximate analysis of biomass feedstock using a muffle furnace (FO410C, Yamato, Japan) was conducted according to Chinese standard GB/T 212–2008 and American standard ASTM D 3172–89(2002). The ultimate analysis was carried out in an CHNS elemental analyzer (vario EL cube, elementar, Germany) on dry ash-free basis. The results of proximate analysis and ultimate analysis of biomass sample are listed in Table S1. The reason why pine sawdust was adopted is that it is one of the most universally used materials for pyrolysis and/or gasification of biomass in

literatures, by which the experimental results could provide practical instruction for the effects of this study on complex biomass feedstock in real-world cases.

The chemicals and reagents employed in this study are displayed as follows:

All chemicals and reagents used in this work were analytical grade without further purification. Nickel nitrate hexahydrate ($Ni(NO_3)_2 \cdot 6H_2O$, CAS: 13478-00-7) and ferric nitrate nonahydrate ($Fe(NO_3)_3 \cdot 9H_2O$, CAS: 7782-61-8) in purity of 99.99% were used as precursors of active metals to provide Ni and Fe content for catalyst synthesis, obtained from Aladdin Biochemical Technology Co., Ltd. (Shanghai, China). The support of catalyst adopted activated alumina (γ-Al_2O_3, Aladdin, 40-60 mesh, CAS:1302-74-5). A water purification system (UPD-I-10T, ULUPURE, Chengdu, China) was employed to supply the deionized and ultrapure water used during experiment.

2.2 Catalyst preparation

In this work, a bimetallic catalyst was prepared through incipient wetness impregnation method to load the active metals Ni and Fe onto support material γ-Al_2O_3, with 15 wt% total metal loading weight ratio and 3:1 Ni-Fe ratio. The ratios were determined considering previous studies because those conditions were decent for catalyst fabrication and performance. Also, this study was meant to investigate the effects of temperature and catalyst on integrated pyrolysis and plasma catalysis system for biofuel production, instead of catalysts screen, design or optimization.

(i) The γ-Al_2O_3 support was processed through pretreatment with incipient wetness volume of pure water according to previously reported method[44]. Then, the specific amount of nickel nitrate hexahydrate and ferric nitrate nonahydrate (i.e. as 3:1 Ni-Fe weight ratio) were added and dissolved in deionized water to prepare precursor solution

in incipient wetness volume of used γ-Al_2O_3. (ii) The nitrate salt solution was gradually dripped into support particles with moderate stirring to make them thoroughly mixed, until all the γ-Al_2O_3 particles were evenly soaked. (iii) The resulting slurry was kept continuously stirring at 60℃ for 2 hr to ensure complete mixture, which was then aged overnight (nearly 10 hr) at room temperature. (iv) Next, the resulting catalyst was dried in oven at 105℃ for 6 hr, following by the calcination in a muffle furnace at 600℃ for 3 hr with 5℃/min heating rate. (v) The catalyst was then sieved to ensure 40-60 mesh particulate form used in experiments. Eventually, the calcined catalyst was reduced in 15 vol% H_2/Ar mixed gas with flow rate of 100 ml/min prior to use (600℃, 3 hr, 5℃/min heating rate). The as-prepared Ni-Fe bimetallic catalyst with γ-Al_2O_3 support after reduction will be known as fresh catalyst hereafter, which is denoted as Ni-Fe/γ-Al_2O_3.

2.3 Experimental system and procedures

The novel integrated pyrolysis and plasma-enhanced catalysis system was mainly designed and assembled based on a two-stage fixed reactor system, illustrated as schematic diagram in Fig. 1. A 700 mm-long quartz tube, with 25 mm in O.D. and 18 mm in I.D., was adopted to achieve serial processes integrating biomass pyrolysis and plasma-catalysis reforming of volatiles in one system. Biomass sample was put into a quartz crucible with a certain amount of quartz wool above, which was hung in the middle of upper stage. Lower quartz tube served as the dielectric barrier to construct a cylindrical DBD plasma apparatus, where plasma can be turned on and off. Accordingly, biomass pyrolysis was accomplished in the top stage, while the bottom stage was applied to carry out plasma-catalysis reforming reaction, where the temperature can be controlled by first and second electric furnace respectively.

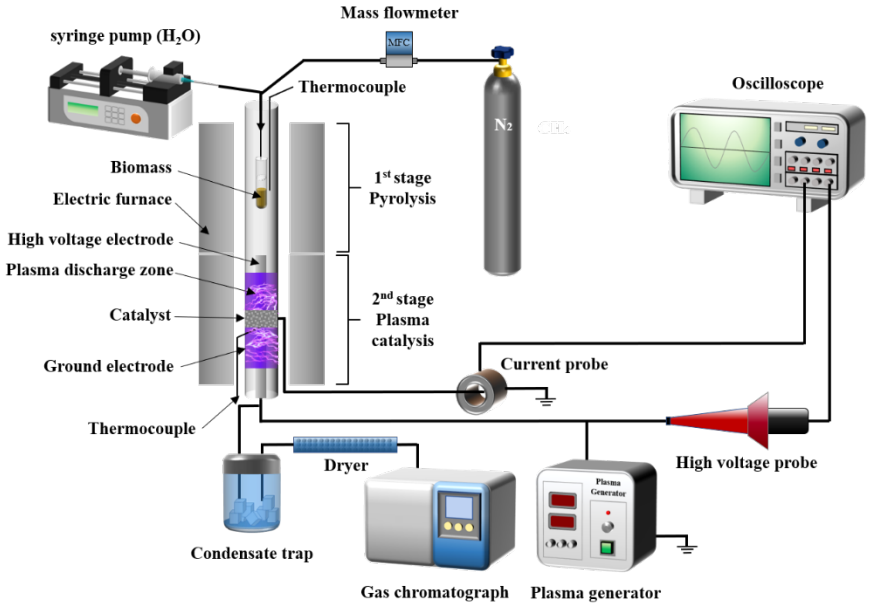

Fig. 1 Schematic diagram of integrated pyrolysis and plasma-catalysis system

For DBD plasma section, the high voltage electrode was served by a 300 mm-long stainless-steel rod with 15 mm in O.D., fixed along with the axis of quartz reactor. Meanwhile, a stainless-steel mesh with 80 mm in length was wrapped around the outer quartz tube to work as ground electrode. Thereby, the plasma can be generated across a 1.5 mm discharge gap inside the reactor, by using an AC sinusoidal high voltage power supply (CTP-2000K, Coronalab., Nanjing, China) with peak-to-peak voltage of 30 kV and frequency of 10 kHz. The applied voltage and current were measured by a high voltage probe (P6015A, Tektronix, US) and a current monitor (2877, Pearson, US) respectively. A digital oscilloscope (MDO 3054, Tektronix, US, 500 MHz, 2.5 GS/s) installed four channels was adopted for electrical signals recording during plasma commissioned. After installing a capacitor (0.47 μF) in series in external discharge circuit, a Q-U Lissajous figure method was applied to obtain the actual discharge power of plasma zone inside the reactor[45, 46]. Q is the measured charge on the external capacitor by a probe, and U is the applied voltage from high voltage probe. Further detailed experimental procedures can be found in S1.2 in supporting information.

2.4 Catalyst characterization and coke determination

The specific surface area, pore volume and pore diameter of fresh and used catalysts were detected by Brunauer-Emmett-Teller (BET) analysis using an instrument of JW-BK200 (JINGWEIGAOBO Ltd., Beijing, China). A Bruker diffractometer (D8 Advance, Bruker Ltd., Germany) and Jade 6 software were used for X-ray diffraction patterns (XRD) analysis to obtain the crystal structure of fresh and used catalysts, with 2θ angle from 10° to 90°. The surface morphology and microstructure of fresh and used catalyst were observed through a field-emission scanning electron microscope (GeminiSEM 500, Carl Zeiss, Shanghai, China), with utilization of energy dispersive X-ray (EDX) for element distribution imaging. The details of morphology characterization for fresh catalyst are shown in Fig. S1, described in supporting information

To determine the coke deposition on the used catalyst, thermo-gravimetric analyzer (SHIMADZU, Japan) was employed for thermogravimetric analysis (TGA), where samples were tested under 75 ml/min air flow at a heating rate of 10°C/min from room temperature to 850°C. Also, an elemental analyzer (vario EL cube, elementar, Germany) was utilized for coke amount measurement. Raman spectroscopy (DXR2xi, Thermo Fisher) was carried out to ascertain the carbon species on used catalyst, with 532 nm laser line as excitation source.

2.5 Definitions

The yield and selectivity of gaseous products (i.e. H_2, CO, CH_4, CO_2 and C_2-C_3 hydrocarbons) were calculated as follows:

$$Y_{product}(mmol/g_{biomass}) = \frac{n_{product}}{m_{biomass}} \quad (1)$$

where $Y_{product}$ is the yield of gaseous products. $n_{product}$ and $m_{biomass}$ represents moles of products in mmol and mass of biomass in g, respectively.

$$S_{product}(\%) = \frac{n_{product}}{n_{total}} \times 100 \quad (2)$$

where $S_{product}$ is the selectivity of produced gases. $n_{product}$ and n_{total} is the moles (in mmol) of specific product and moles of total gaseous products, respectively.

When employing plasma and catalyst for reforming process, the synergy capability (SC) of plasma-catalysis system can be calculated as follows[16, 47]:

$$SC\ (\%) = \frac{Y_{PC} - Y_P - Y_C}{Y_P + Y_C} \times 100 \quad (3)$$

where SC represents the synergy capability. Y_{PC}, Y_P and Y_C denotes the resultant yields attained in the case of plasma-catalysis, plasma alone and catalyst alone mode, respectively.

3. Results and discussion

3.1 Roles of temperature and catalyst in integrated system

The major concern of this study is to investigate the roles of temperature and catalyst of novel hybrid system on biomass volatiles reforming, where the upper pyrolysis stage was used to produce volatile matters from biomass feedstock. Thereby, according to the TGA results of pine sawdust in Fig. S2, the volatile matter derived from feedstock could be completely released at around 650℃. Then, we tested the effect of pyrolysis temperature on the products output and distribution, plotted as Fig. S3. Only subtle difference of H_2 yield between 650℃ and 750℃ can be observed, but presenting a distinct increase compared with that at 550℃. As a result, 650℃ was fixed as 1st stage temperature for pyrolysis in the following experiment from the H_2-enhancing and energy-saving points of view.

3.1.1 Influence of plasma discharge power

Non-thermal plasma was believed to be a cogent tool for process enhancement for example, tar reforming[34]. First, experiments without catalyst and steam were carried out to verify the efficacy of varying plasma discharge power, where the reforming stage was fixed at room temperature (i.e. without external heating by electric furnace) to minimize interference to plasma action. Herein, a standard Q-U Lissajous figure method was adopted to calculate the actual plasma power in discharging zone[45, 46]. In this case, the value can reflect the real power inside reactor by eliminating other accessories consumption.

As can be seen from Fig. 2, introducing plasma was clearly able to promote the yields of all gaseous products, compared with that in heating-only condition (i.e. 0 W discharge power). Especially, as for H_2 and CO production, positively varying the plasma power exhibited more prominent enhancement. With the elevation of power input to 15 W, H_2 and CO yield increased from 0.81 and 1.02 mmol/g to 4.07 and 4.34 mmol/g, respectively, more than 4 times higher than that before turning on plasma. While only limited growth of other gases, including CO_2, CH_4 and C_2-C_3, could be observed with plasma on and rise of power. Whereas, introducing plasma was still not able to improve the H_2 production to a considerable level compared to traditional researches using thermochemical route (e.g. 18.7 mmol/g at 800℃ with Ni-based catalyst)[48]. With respect to the selectivity of different gas composition shown as curves in Fig. 2, the same positive trend of H_2 and CO could be obtained as the plasma power turning up, resulting in a reasonable increase for syngas selectivity. Inversely, CO_2 composition among gaseous products kept decreasing with discharging power.

Those results are mainly ascribed to the decomposition and reforming of tar and other

volatiles from pyrolysis stage. After plasma ignition, the production of energetic electrons can contribute to the cleavage of C-C and C-H bonds in hydrocarbon compounds to generate reactive species, motivating decomposition and reforming for gases yields. As turning up the discharging power, increasingly abundant electrons resulted from enhanced microdischarges can provide more reaction channels and reactive species to further facilitate the above process. As a result, the yields and selectivity of H_2 and CO can be increased by introducing plasma and rising power even without heating input. But it was still not favorable enough compared with conventional catalytic process in high temperature. Besides, randomness of plasma reforming bringing about relatively unsatisfactory H_2 selectivity was an issue to be addressed. Considering the specific energy consumption and operational security, it is not advisable to increase power input excessively. Therefore, a power input of 15 W was determined for the following plasma experiments.

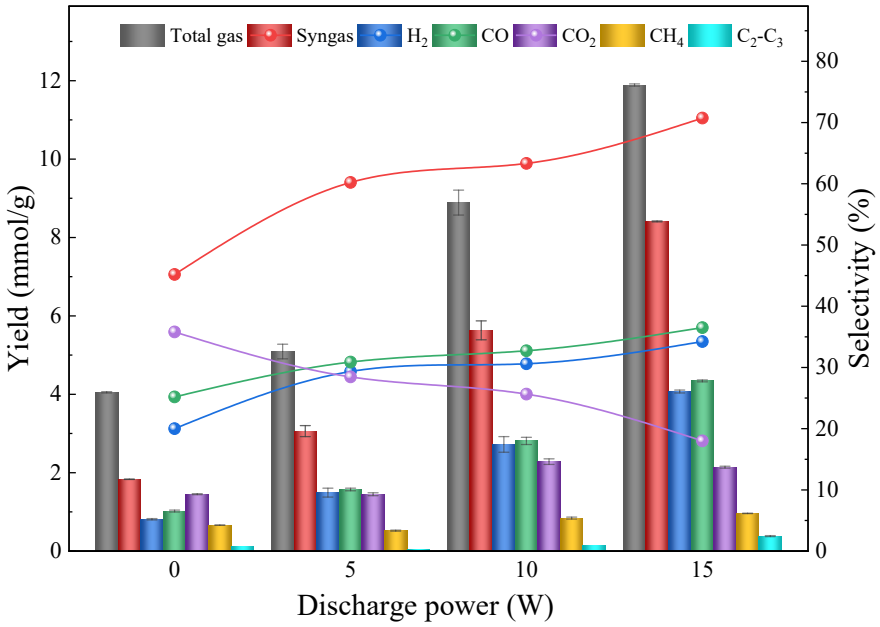

Fig. 2 Effect of discharge power on yields and selectivity of gaseous products (2nd reforming room temperature; no steam; no catalyst)

3.1.2 Influence of steam input

It is of great significance to ascertain the effect of steam input on this novel integrated system since, in practical engineering of biomass pyrolysis/gasification, there is always non-negligible amount of moisture content. Previous studies attested the positive function of steam on H_2 production during plasma reforming process[49]. Herein, we investigated the influence of varying steam liquid hourly space velocity (LHSV), from 0 to 10 ml/h/$g_{biomass}$, on the plasma system performance without catalyst at room temperature.

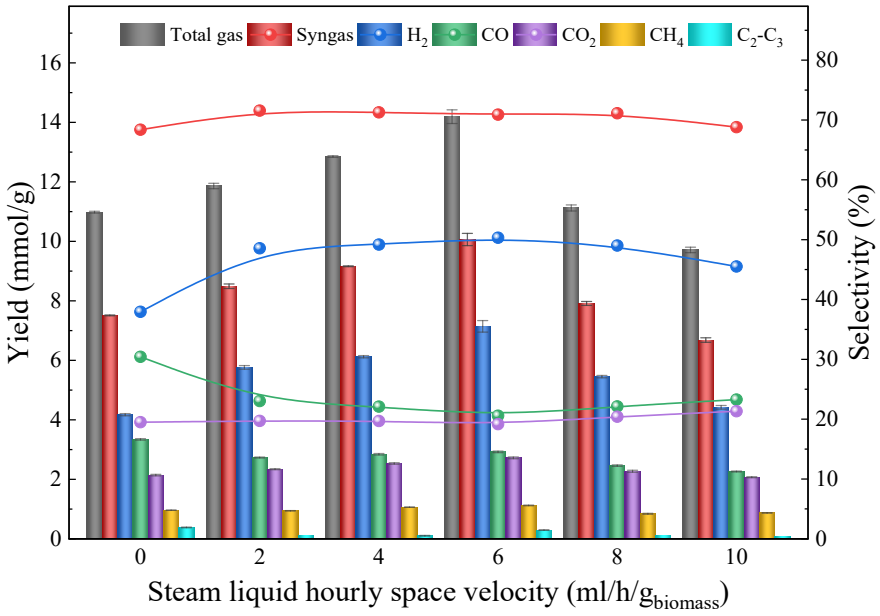

Fig. 3 Effect of steam LHSV on yields and selectivity of gaseous products (2nd reforming room temperature; discharge power 15 W; no catalyst)

The results of varying LHSV effect on the yields and selectivity of gaseous product are depicted as Fig. 3. In comparison of effectiveness with steam LHSV of 2 ml/h/$g_{biomass}$ and with plasma-only reforming (0 ml/h/$g_{biomass}$), production and selectivity of H_2 augmented from 4.17 mmol/g and 37.95% to 5.76 mmol/g and 48.55%, respectively. This demonstrated that a considerable promotion of H_2 yield and

selectivity can be achieved after injecting steam into reforming process. The improvement can be attributed to the generation of H and OH radicals after introducing water into discharge zone, resulted from water dissociation by energetic electrons and water collision with excited nitrogen species in carrier gas. And H_2 can be generated by recombination of H radicals. The detail processes are presented as R1-R4. Those radicals with high activity and strong oxidizing property can contribute to the enhancement of H_2 production by means of creating new reaction routes for hydrocarbon conversion and tars destruction. Notably, the CO yield and composition percentage exhibited a reduction phenomenon after steam input. It can be explained by the process that introducing steam can also increase H_2 production through pathway of water gas shift (R5), where the CO could be consumed.

$$H_2O + e \rightarrow H + OH + e \quad \text{(R1)}$$

$$N_2 + e \rightarrow N_2^* + e \quad \text{(R2)}$$

$$N_2^* + H_2O \rightarrow N_2 + OH + H \quad \text{(R3)}$$

$$H + H \rightarrow H_2 \quad \text{(R4)}$$

$$CO + H_2O \rightarrow CO_2 + H_2 \quad \text{(R5)}$$

$$H_2O + e \rightarrow H_2O^- \quad \text{(R6)}$$

However, as the variation tendency in Fig. 3, the monotonic growth of H_2 production could not always be acquired through continuously increasing steam input. The H_2 yield initially rose by almost double (from 4.17 to 7.39 mmol/g) when injecting steam LHSV from 0 to 6 ml/h/$g_{biomass}$, followed by a decline trend (from 7.39 to 4.42 mmol/g) with constant increase of steam flow rate (from 6 to 10 ml/h/$g_{biomass}$). The plateau of results indicated that an optimal steam LHSV of 6 ml/h/$g_{biomass}$ could be obtained for maximum

H_2 production and selectivity in 7.39 mmol/g and 50.37%, respectively. It implied that excess steam input brough about opposite effect to performance of plasma reforming zone, which conforms with results of other works reported[49]. This phenomenon could be imputed to quenching of energetic electrons and reactive species, such as R3 and R6, which is resulted from the attachment to steam molecules (with electronegativity). Balance between two opposite effects, thus, orients the influence of steam input on system performance, where positive effect is from the H and OH generation for various reaction pathways, while water attachment contributes to negative one. Besides, not much of a boost to gas composition ratios is mainly due to intrinsic nature of plasma in low selectivity. Consequently, we adopted steam LHSV in 6 ml/h/$g_{biomass}$ in the subsequent experiments. Similar steam input optimization is also recommended when applying the plasma reforming in practice with appropriate making use of moisture content in actual bio-energy engineering.

3.1.3 Influence of temperature

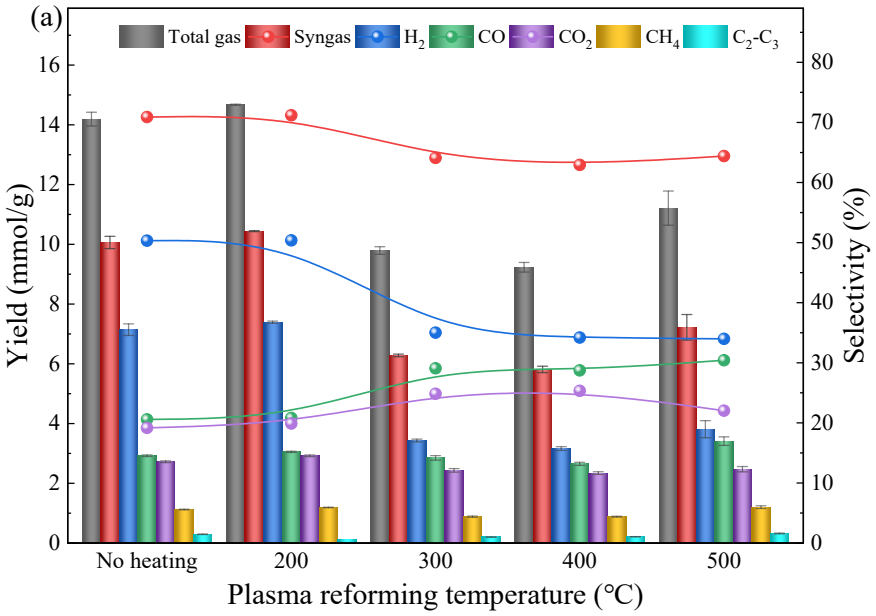

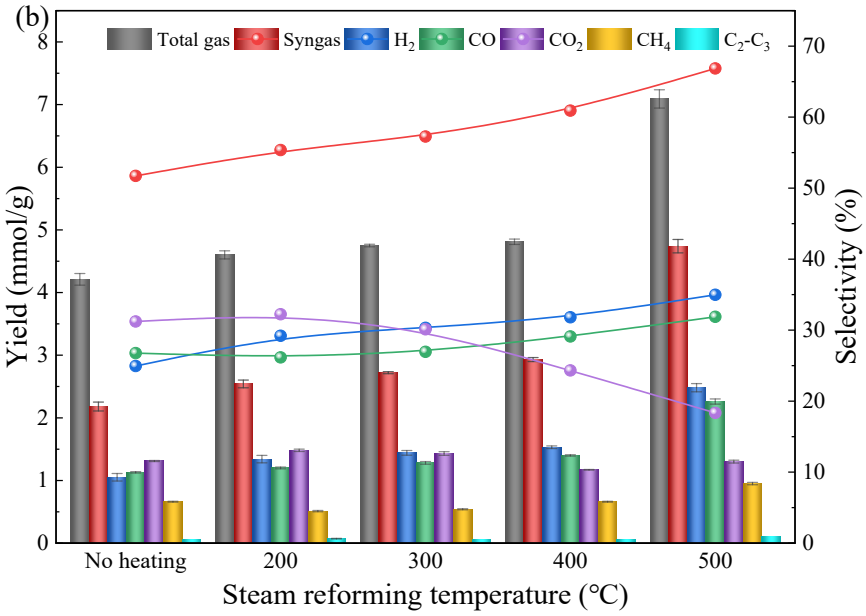

Fig. 4 Effect of reforming temperature (a) with plasma and (b) without plasma on yields and selectivity of gaseous products
(Discharge power 15 W if required; steam LHSV 6 ml/h/gbiomass; no catalyst)

Temperature is a predominant factor not only to catalytic reforming process, but to plasma performance according to previous works reported[50]. Experiments were carried out to tell the specific influence rule of imposed temperature on integrated system with plasma and steam injection, from ambient temperature (i.e. no heating) to 500°C. According to the results illustrated in Fig. 4a, temperature of 200°C conduced to the optimal yields of all gaseous production including H_2. The output of total gas, H_2 and CO produced attained 14.67, 7.39 and 3.05 mmol/g, respectively. Interestingly, a comparable outcome for example, total gas, H_2, and CO production as 14.19, 7.14 and 2.92 mmol/g, respectively, can be obtained without heating input. This can be explained by the self-heating effect derived from discharge of plasma, which can elevate the temperature of reactor to 100°C to hundreds of degrees varying from different specific energy input[51-53]. Liu et al. reported that higher temperature could help to the thermal motion and resultant interactions of free radicals and active species, thus

increasing toluene conversion when rising temperature from 200℃ to 300℃[36]. Accordingly, the attenuated reforming process resulted from lower temperature may be responsible to slight decline of H_2 and other gases without heating compared with those at 200℃.

Further, Fig. 4a displays the selectivity of different gaseous products and their variation trends along with temperature growth. As the consistent results with above, almost identical selectivity of gases was maintained both when no heating and 200℃. Continuously elevating temperature leaded to a slight drop selectivity of H_2 and a rise of CO. It is because the overall gaseous production decreased when rising temperature from 200℃ to 400℃ and then went up with the temperature increasing from 400℃ to 500℃, which disagreed with the consequences of conventional reforming process in literatures[54]. These results reveal that preferable performance of H_2 production could be achieved by plasma reforming process either without heating or with adequately high temperature. The augments of temperature may exert varying influence on those two pathways, giving rise to different H_2 production as well as other gaseous products. Additionally, based on the results, a new pathway for enhancement of H_2 yield from biomass pyrolysis can be constructed employing plasma at ambient temperature without heating input to avoid extra energy consumption.

It can be acknowledged from above that plasma-assisted reforming can be considered superposition of two individual processes, namely, plasma-only and heating-only reaction. Those two approaches could respond dissimilarly to temperature variation for the reforming performance of system. Hence, to further probe into the specific role of temperature in plasma reforming reaction, experiments at varying temperature were conducted under the circumstance of plasma blanking. As plotted in Fig.4b, consistent variation trends of H_2 yield with were obtained. Those findings indicate that enhanced

H_2 production and higher selectivity can be attained through augmenting reforming temperature, which is also advantageous for promoting the syngas and total gas yield. This result is also consistent with previous studies reported. Because, from thermodynamics point of view, equilibriums of endothermic reactions can be motivated to move forwards for more yields of products, such as thermal cracking, hydrocracking, Water-Gas reaction (R7), Boudouard reaction (R8) and Steam-Methane reaction (R9), etc. As for kinetic dynamics, increasing temperature can improve the rates of reaction occurring in reforming stage, leading to higher output of gaseous products, by which more H_2 can be acquired. In addition, the reduced CO_2 yield and selectivity can be ascribed to the promoted rate of Boudouard reaction as shown in R8. And relatively higher yield and selectivity of CO compared with those of H_2 at room temperature was because of inadequate WGSR (R5) resulted from incomplete steam vaporization and function without heating.

$$C + H_2O \rightarrow CO + H_2 \quad \text{(R7)}$$

$$C + CO_2 \rightarrow 2CO \quad \text{(R8)}$$

$$CH_4 + H_2O + \rightarrow CO + 3H_2 \quad \text{(R9)}$$

When combining the results of Fig. 4a and b, it can be observed that the H_2 production declined by 42.8% from the highest yield at 200℃ to the lowest at 400℃, with a similar drop of selectivity (as Fig. 4a), which was conflicting with the tendency of positive effect of temperature presented in Fig. 4b. Therefore, it uncovers that, at relatively low temperature, plasma reaction system is advantageous to produce higher H_2 yield with acceptable selectivity, whilst if turning the plasma off, more satisfactory performance can be obtained by temperature elevation. To further explore the relationship between temperature and plasma reforming, we worked out the respective

contribution of plasma and heating on the yields of total gas, syngas and H_2 at varying temperature, illustrated as Fig. 5. The sole plasma contribution could be obtained through deducting the product yields of steam reforming process in Fig. 4b from those of reforming process with plasma as showed in Fig. 4a. By doing so, we can eliminate the influence derived from heating on reaction performance of reforming with plasma assistance, which allow a rational comparison of the role of plasma and heating in our system.

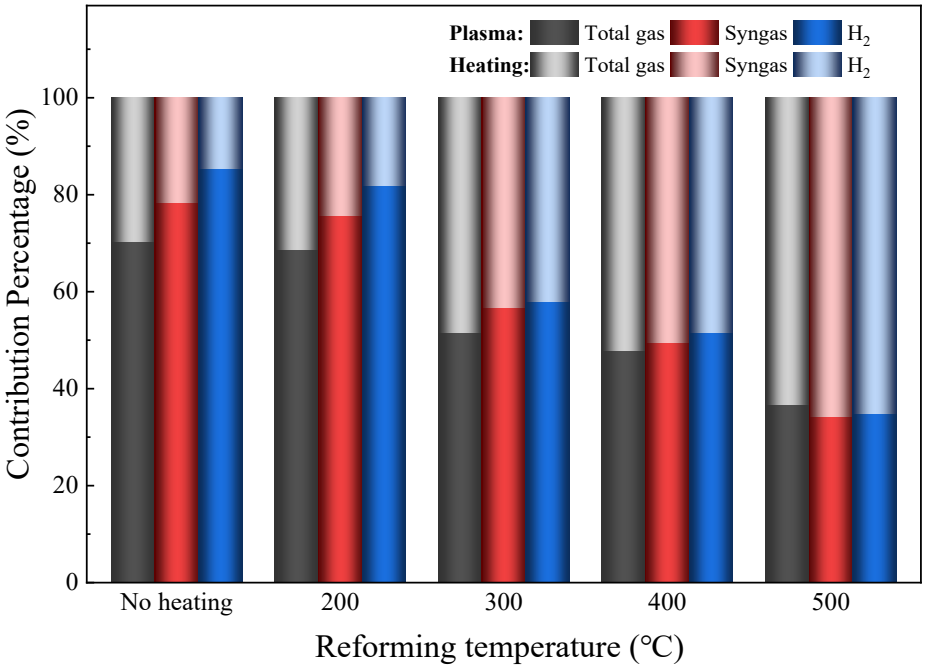

Fig. 5 Plasma and heating contribution to yields of total gas, syngas and H_2 (Heating contribution was obtained directly from results in Fig. 4b; plasma contribution was calculated by subtracting the heating contribution from plasma reforming data in Fig. 4a)

According to the contribution and variation in Fig. 5, an obvious drop trend of contribution from plasma only can be observed when the temperature was continuously lifted. The most noticeable tendency can be found in blue bars representing plasma and heating contributions to H_2 production varying from temperatures, where the percentage of plasma contribution markedly fell off from 85.29% to 34.91% as temperature rising from ambient condition to 500℃. Besides, the plasma-enhanced

effect contributed to H_2 yield was even more prominent to other gaseous products. It can be concluded that the H_2 production mainly derives from plasma-enhanced effect at lower temperature or without heating condition. Whilst, at higher temperature, heat-induced effect is principally responsible for upgrade of reforming performance. What is additionally noteworthy in Fig. 5 is that the percentages of plasma contribution to gaseous products including H_2 at ambient condition were the highest and all slightly higher than those at temperature of 200℃. It is because the actual temperature in 2nd stage without heating was slightly lower than 200℃, also proving the abovementioned resultant temperature caused by plasma heat effect. Above findings indicates that the effectiveness of reforming under plasma assistance could be impaired when inputting exogenous heating or in elevated environment temperature.

The similar detriment on the non-thermal plasma performance from higher temperature was also reported in other related works. On the one hand, rising temperature may alter the reaction process under plasma environment. For instance, Saleem et al. adopted toluene as surrogate of tar to investigate the effect of CO_2 on its conversion in a DBD plasma system. They reported a slight decline of toluene conversion rate when rising temperature, mainly attributed to accelerated recombination between CO and O radicals, that is, plasma-induced reactive species was reduced due to heating[55]. On the other, characteristics of plasma discharge may also be depressed by temperature elevation. According to the study by Liu et al. on dry reforming of biogas and toluene using non-thermal plasma, a dramatic drop of toluene conversion efficiency was found after increasing temperature from 400℃ to 500℃. A reduced electroinsulating property of quartz caused by local thermal runway at high temperature was proposed as the reason, thereby decreasing reactive species derived from the dissociation of N_2 and O_2, which leaded to an inferior overall performance[36].

In a similar system, Xiao et al. claimed a promoted gas and oil production with the increase of temperature, which mainly ascribed to the decreased formation of wax[50]. However, they failed to recognize the unlike effects of temperature on the heating process and plasma process, because the improved gases production may come from the decomposed wax but the plasma discharge still was impaired.

According to previous literature about plasma characteristics research, at elevated temperature under external heating input, lower breakdown voltage is required for plasma zone to generate same discharge power, which can be also interpreted via Paschen's law[56]. Thus, the mean electric field (E) and mean reduced electric field (E/N) are accordingly minished with reduced peak-to-peak voltage across the electrodes as temperature growth[45, 57]. It could directly impair the energetic electrons, then weakening the cleavage of tars and lessening the induced active species, which ultimately bring about inferior performance of plasma-assisted system at high reforming temperature. As a result, the influence of temperature conditions on performance of integrated pyrolysis and plasma-assisted reforming system without catalyst is dependent on the trade-off between two opposite effects on the reaction in 2^{nd} stage: i) promoted H_2 production derived from strong heating-only effect at higher temperature and ii) attenuated H_2 production caused by impairment to plasma-only performance with extra heat input at elevated temperature. Herein, considering the specific energy consumption and experimental performance, no external heating at ambient condition is proposed as optimum for H_2 and syngas production in 2^{nd} stage of integrated pyrolysis and plasma reforming without catalyst.

3.1.4 Influence of catalyst packing

Packing catalysts into the plasma discharge gap is turned out to be a rational mean

for improvement of catalytic performance, which is mainly ascribed to the synergistic effects between catalyst and plasma. A hotspot of recent research works is to develop and design the catalyst systems with strong synergy and high effectiveness in plasma zone at relatively low temperature, while investigation into performance and mechanism of plasma-catalysis synergistic system at varying temperatures is still scarce. On this basis, we employed as-prepared bimetallic 3:1 Ni-Fe/γ-Al_2O_3 in plasma reforming stage to build the integrated pyrolysis and plasma-catalysis system, by which the performance and role of catalyst on H_2 production at different temperatures could be comprehensively studied, as well as the synergy effects.

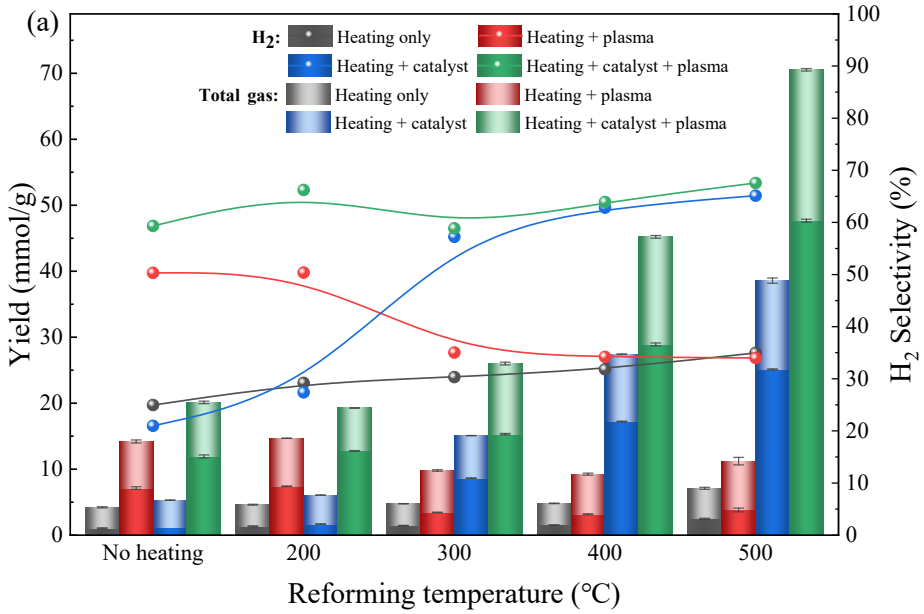

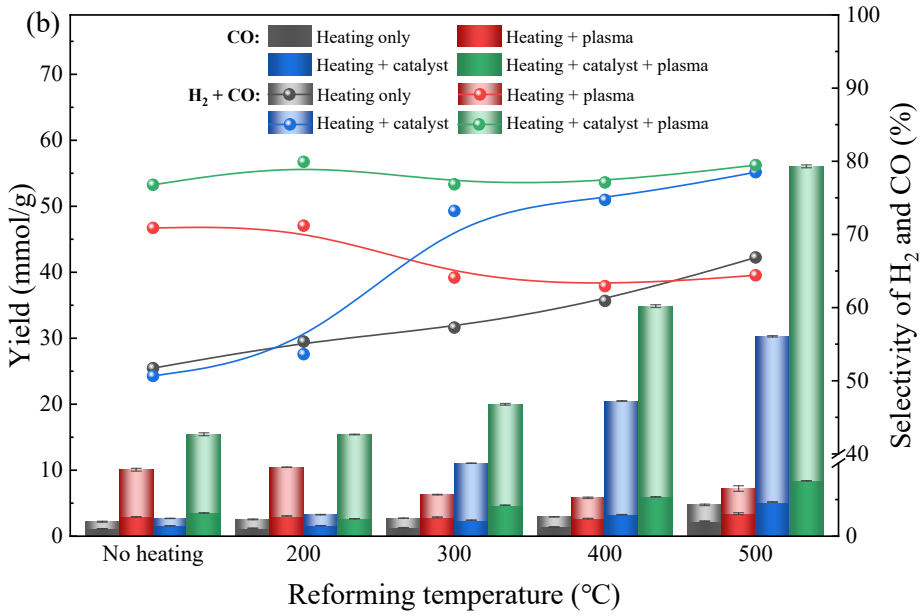

475

476 Fig. 6 Effect of catalyst on (a) yields of H_2 and total gas and H_2 selectivity, and (b) yields of
477 CO and H_2 and selectivity of CO + H_2 at varying reforming temperatures
478 (Discharge power 15 W; steam LHSV 6 ml/h/$g_{biomass}$; catalyst 3:1 Ni-Fe/γ-Al_2O_3 if required)

479 Fig. 6 depicts the gases yields (i.e. total gas, H_2, CO and H_2+CO) and composition
480 variation (i.e. H_2 and H_2+CO) after packing catalyst into 2nd stage both in the presence
481 and absence of plasma discharge. Besides, the resultant yield and selectivity of CO_2,
482 CH_4 and C_2-C_3 at varying temperature in different modes are also provided as Fig. S4.
483 The corresponding results under conditions of heating only and plasma reforming are
484 also illustrated in figure for the sake of visualized comparison, of which the data is
485 extracted from Fig. 4. According to Fig. 6, there was an obvious promotion in terms of
486 total gas yields, including H_2 and CO, when packing bimetallic catalyst into plasma
487 zone no matter what the reforming temperature was set. It indicates that plasma-
488 catalysis reforming outperforms other three modes at all temperatures. After
489 introducing the catalyst into reforming process at ambient temperature as shown in Fig.
490 6a, the growth in yields of total gas and H_2 was only 1.35 mmol/g and 0.06 mmol/g
491 respectively, showing a nearly unserviceable effect of catalyst due to no extra heating.

However, with plasma and catalyst, the total gas and H_2 production increased near fivefold and more than elevenfold respectively, compared with those under heating only case. Surprisingly, we can observe that H_2 production from plasma-catalysis system (11.93 mmol/g) was even higher than that from adding together of outcomes by catalyst only (1.11 mmol/g) and plasma only (7.14 mmol/g) mode, clearly demonstrating that there is a synergistic effect when packing catalyst into plasma zone. This plasma-induced synergy is also consistent with other different plasma-catalysis system reported before[46, 47]. Also, the selectivity of H_2 derived from plasma-catalysis mode was the highest in 59% under this condition, which shows that the catalyst come into play when working together with plasma discharge.

As presented in Fig. 6a, b and Fig. S4, all gaseous products were increased along with the elevation of temperature in the presence of Ni-Fe/γ-Al_2O_3, owing to its promoted catalytic activity at higher temperature as conventional thermochemical conversion. At relatively lower temperature below 300℃, performance of applying plasma (red bar) was obviously better than that of using catalyst only (blue bar), owing to the incompetence and inefficiency of catalysts in lower temperature. Whereas, with reforming temperature increasing, the production and selectivity of H_2 with catalyst only gradually exceeded those with plasma only, which again demonstrates two counter effects of temperature rise on the performance of heating-plasma and heating-catalyst reforming processes. When focusing on the variation of total gas and H_2 yields under plasma-catalysis system (green bar), there was a significant climb in production with temperature elevating. The same trends can be also discovered in terms of syngas and CO production, indicating dissimilar roles played by temperature between only applying plasma and adopting plasma-catalysis mode. It can be explained by the fact that higher temperature with extra heating input is always conducive to promote the

performance of reactions with catalyst involved, which agrees with conventional thermochemical processes reported[25].

According to Fig. 6a, 47.65 mmol/g and 70.53 mmol/g of H_2 and total gas yields was obtained respectively after rising temperature to 500℃ under plasma-catalysis system, which is the optimal production capacity in this study. It is worth noting that, compared with effect of plasma reforming (red bar) at 500℃, packing the Ni-Fe/Al_2O_3 into plasma zone prominently augmented production of H_2 and total gas by more than 11 folds and 5 folds, respectively. However, when without extra heating, plasma-catalysis system can only enhance around 67% and 42% yields of H_2 and total gas. It can be deduced that reforming process enhanced by plasma only works well in lower temperature owing to detrimental effect of heating on plasma characterizations, while plasma-catalysis system could outperform with exogenous heating input due to catalyst activation at higher temperature. H_2 and H_2+CO selectivity in case of different modes is also plotted in Fig. 6a and b, which demonstrates two opposite variation trends under plasma alone and catalyst alone mode along with increasing temperature. Whereas, there was no significant difference as elevating temperature in case of plasma-catalysis system. It is because the plasma reforming is generally a process of random breakage and recombination between molecules with low selectivity[27]. Thus, the property of catalyst acts a dominant role at higher temperature to determine the upper limit of reaction selectivity, where the plasma characterization under plasma-catalysis system could be partially inhibited. Even so, the highest selectivity of H_2 and H_2+CO in this work was attained in case of plasma-catalysis system at reforming temperature of 500℃, which reached at about 68% and 80% respectively, demonstrating a satisfactory condition and outcome after introducing catalyst into plasma process.

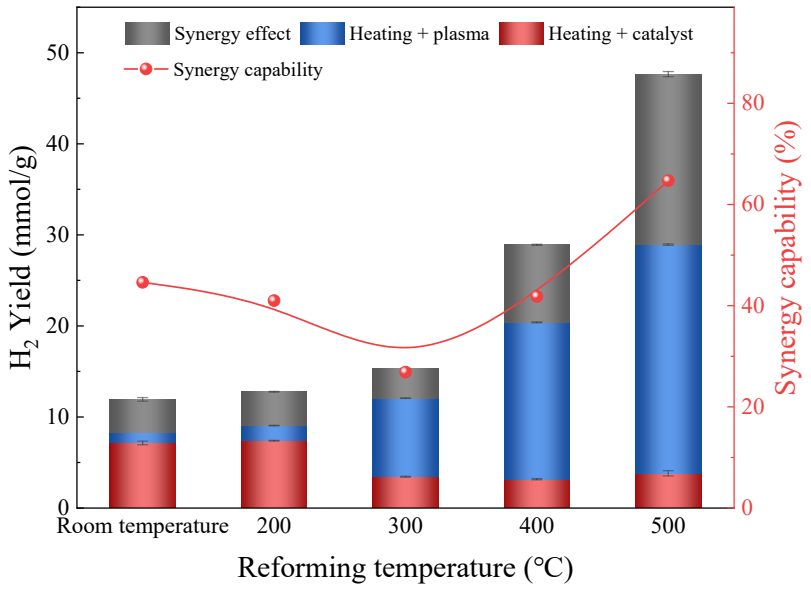

Fig. 7 Synergy effect and capability for H_2 production in case of plasma-catalysis system (Synergy effect was obtained by subtracting yields of plasma alone and catalyst alone from that of plasma-catalysis mode)

Interestingly, we can also observe that the H_2 and total gas yields at 500℃ (47.65 mmol/g and 70.53 mmol/g) resulted from plasma reforming with catalyst were all higher than the sum of production from catalyst only (25.12 mmol/g and 38.57 mmol/g) and plasma only (3.81 mmol/g and 11.21 mmol/g) mode, shown as Fig. 6a and Fig S4. Thus, it reasonably demonstrates a synergistic effect between plasma and catalyst for reforming process, which was similarly recognized at all temperature conditions in our study. Besides, as can be seen from Fig. 7, this synergy capacity calculated by Eq. 4 is more prominent at higher reforming temperature. Not only could the function of catalyst be stimulated via elevated temperature to a greater extent, but the plasma discharge could interact with catalyst to induce the synergy effect for further overall performance promotion, even though the plasma characterization can be impaired by extra heating. The reason why there was a low synergy capability at 300℃ is that this temperature condition cannot activate catalyst enough and antagonizes the plasma

discharge. Therefore, in this plasma-catalysis system, the role of catalyst is the most dominant at higher temperature, rather than the plasma that plays an assistant for process enhancement. Consequently, both the H_2 yield and selectivity obtained can be fully capable to compete with that from conventional thermochemical process (generally 800℃-1000℃), but at a relatively low temperature (500℃). These advantageous effects endow this novel system with promising application prospects as its competitive performance in low temperature and energy consumption.

3.2 Effects of integrated pyrolysis and plasma-catalysis system on tar elimination

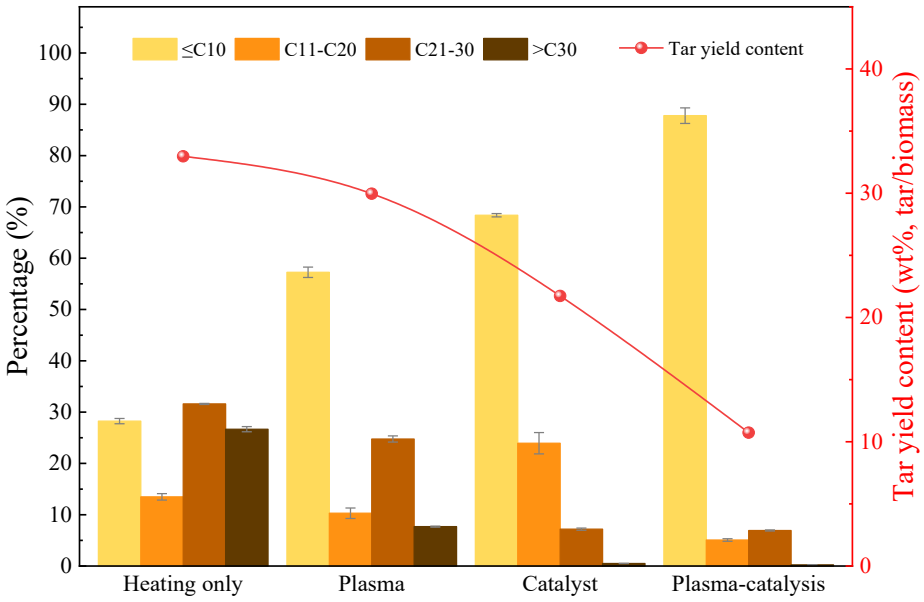

Fig. 8 Effect of integrated pyrolysis and plasma-catalysis on tar composition grouped by carbon number and tar yield content
(Reforming temperature 500℃; discharge power 15 W if required; steam LHSV 6 ml/h/$g_{biomass}$; catalyst 3:1 Ni-Fe/γ-Al_2O_3 if required)

During biomass pyrolysis/gasification, tar is considered a bottleneck for further application and commercialization, because it can cause the blockage of downstream equipment, termination of process and particularly reduction of energy efficiency. In this context, we studied the performance of integrated pyrolysis and plasma-catalysis

on tar elimination from biomass volatiles during the H_2 production. First, the four different reforming mode heating, plasma, catalyst and plasma-catalysis were carried out to determine the condensed tar content formation in the products. As plotted by curve in Fig. 8, tar yield under steam reforming at 500℃ was significantly high, which was more than 32wt% of biomass, with evident brown oil sticking to the inner wall of reactor and condenser. It is an important reason why the gases production was the least in this mode, which could be attributed to the low reforming temperature. According to previous report, the resultful decomposition of tar compounds by thermal cracking could only be achieved with high temperature more than 1100℃[58]. Plasma discharge can moderately reduce the tar content by 3 wt% compared with that of heating only mode at 500℃. It is because, as discussed above, the plasma characteristics could be impacted increasingly with the temperature elevation, leading to the depression of tar removal performance. When employing catalyst at this temperature, the condensed tar was cut down to no more than 22 wt% of feedstocks under the action of thermal cracking and catalytic reforming. The integrated system with plasma-catalysis synergy distinctly outperformed others on the effective tar elimination for three times more than that of heating only, which is attributed to the thermal cracking and, most importantly, reforming process under the synergistic catalysis effects from collaboration of bimetallic catalyst and plasma.

The collected tar samples from different experimental modes were analyzed using GC-MS for detection of various compounds and structures, shown as Fig. S5. Although the actual specific tar compounds cannot be simply determined by peak area of GC-MS results, we can still carry out rational comparison of relative content variation among different samples due to the identical mass injected. Owing to the complexity of products in biomass tar, it is hard to discuss every single the compounds detected

separately. Therefore, we grouped the GC-MS results of different modes by their carbon number as ≤C10, C11-C20, C21-C30 and >C30, respectively, presented in Fig. 8. From the Fig. S5, it is clearly that the detectable peak numbers were significantly reduced when applying the plasma-catalysis system, compared with others. In this study, tar derived from the heating only mode was mainly the primary biomass tar formed in pyrolysis stage containing aromatics, long-chain hydrocarbons and oxygenated hydrocarbons, which is resulted from the insufficient temperature at 500℃ for effective thermal decomposition. Those results are also in line with literatures reported[34, 40]. Surprisingly, introducing plasma-catalysis process significantly cut the tar proportion in C11-C20 and C21-C30 down to 5.07% and 6.92%, respectively. And scarcely any tar compounds with carbon number more than 30 was detected in this condition. It can thus be illustrated that heavy condensed tar molecules hard to remove at low temperature can be effectively decomposed by plasma-catalysis, leading to the overall decline of average molecular weight of tar produced.

For integrated pyrolysis and plasma-catalysis system, on the one hand, the tar may be eliminated by homogeneous conversion under plasma effect. The reactive species in plasma zone, for example, energetic electrons, OH^*, O^* and N_2^*, etc., could help to cleavage of chemical bonds in tar compounds and generation of gases and light hydrocarbons through collision and recombination. On the other, with plasma discharge assistance, the catalyst could be functionalized and activated for the decent heterogeneous reforming of tar to smaller molecular products even under relatively low temperature. Besides, the synergistic effect can further enhance the performance of plasma-catalysis on tar elimination and reforming to facilitate higher gaseous products yields from biomass, which has been discussed above. A few studies investigated and confirmed the efficiency using plasma-assisted catalysis process for the conversion of

tar model compound such as toluene[34]. However, real tar elimination during biomass pyrolysis may be in different case because of its high complexity than toluene. This study demonstrates the proved superiority of integrated pyrolysis and plasma-catalysis for biomass tar elimination during H_2 production. It can also be revealed that plasma-catalysis has promising application for upgrading existing biomass pyrolysis/gasification technology owing to its ability for decomposition of heavy tars at mild condition.

3.3 Lifetime analysis of integrated pyrolysis and plasma-catalysis system

3.3.1 system stability

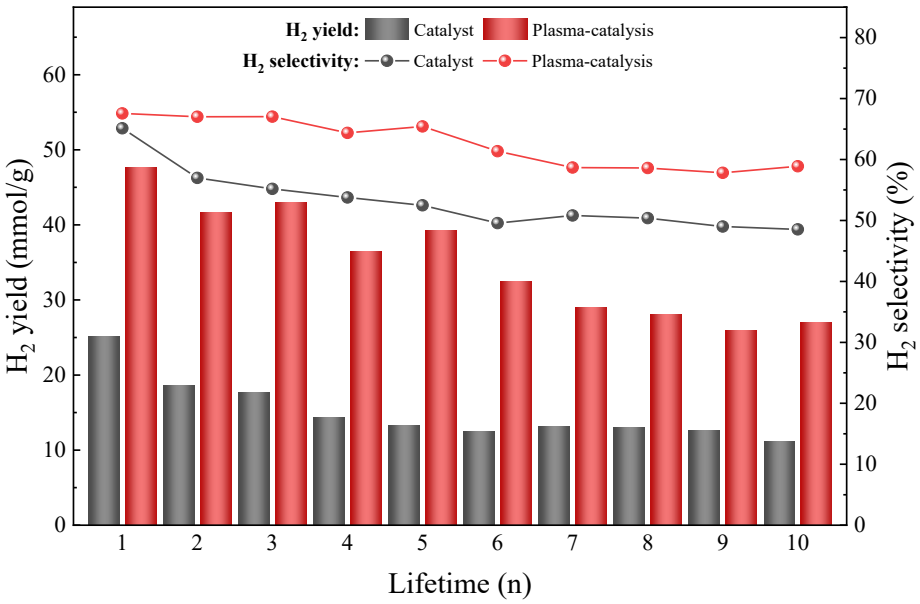

Fig. 9 Stability study for yield and selectivity of H_2 under catalyst only and plasma-catalysis (Reforming temperature 500℃; discharge power 15 W if required; steam LHSV 6 ml/h/$g_{biomass}$; catalyst 3:1 Ni-Fe/γ-Al_2O_3 if required)

To further discuss the practical performance of integrated pyrolysis and plasma-catalysis system, the lifetime analysis experiments for 10 cycles at reforming temperature of 500℃ were conducted under the condition with catalyst and plasma-

641 catalysis, respectively. Fig. 9 depicts the results of H_2 yield and selectivity varying from
642 the increasing experiment cycles, which was under optimal experimental conditions
643 with catalyst and plasma-catalysis reforming processes. With catalyst action, the yield
644 and selectivity of H_2 markedly dropped from 25.12 mmol/g and 65.13% to 18.64
645 mmol/g and 56.98% after the first cycle, respectively, which could be attributed to the
646 rapid deactivation of catalyst. After 10 cycles, the H_2 production and selectivity under
647 sole catalyst effect can be observed for a significant decay to only 11.16 mmol/g and
648 48.54%. The similar results can be found in other reports[59]. This severe performance
649 degradation can be explained by prominent deactivation of Ni-based catalyst, which is
650 caused by accumulated coke deposition, catalyst blockage by tar and probable sintering
651 of active phase.

652 As for the case of introducing plasma-catalysis into reforming process, fluctuated
653 reduction within acceptable range can be observed in the first 5 cycles. The production
654 of H_2 decreased by 17% to 39.28 mmol/g, which was around 3 times higher than that
655 of result from catalyst only after identical experimental cycles. Besides, no obvious
656 decline of the H_2 composition in gaseous products could be incurred after 5 cycles. Then,
657 the downward tendency represented for H_2 yield and selectivity began to level off, of
658 which the timing significantly later than that for catalyst only. After 10 cycles, the
659 production and selectivity eventually decreased to 26.97mmol/g and 59%, respectively,
660 which still shows distinct advantages. This optimized consequence is mainly ascribed
661 to the alleviated catalyst deactivation under plasma assistance. The generated energetic
662 electrons and short-life active species could give rise to the bombardment and complex
663 interaction, where the carbon deposition and heavy tars could be restrained, so that the
664 catalyst could work well under discharge environment after several cycles. It is in line
665 with the effect of plasma-catalysis reported previously[29, 60]. In addition, the plasma

666 can also help to suppress the sintering of active metals for better dispersion when
667 prolonged operation. Therefore, compared with catalyst only mode, the synergy
668 between plasma and catalyst can assist to mitigate catalyst deactivation and avoid the
669 rapid termination of system

670 3.3.2 Effect of plasma on system lifetime

671 To further understand stability performance of plasma-catalysis than catalyst only
672 mode, the critical effects of plasma on system lifetime should be elaborated in catalyst
673 respect. It is because the synergistic promotion between catalyst and plasma discharge
674 is the key for the overall performance improvement.

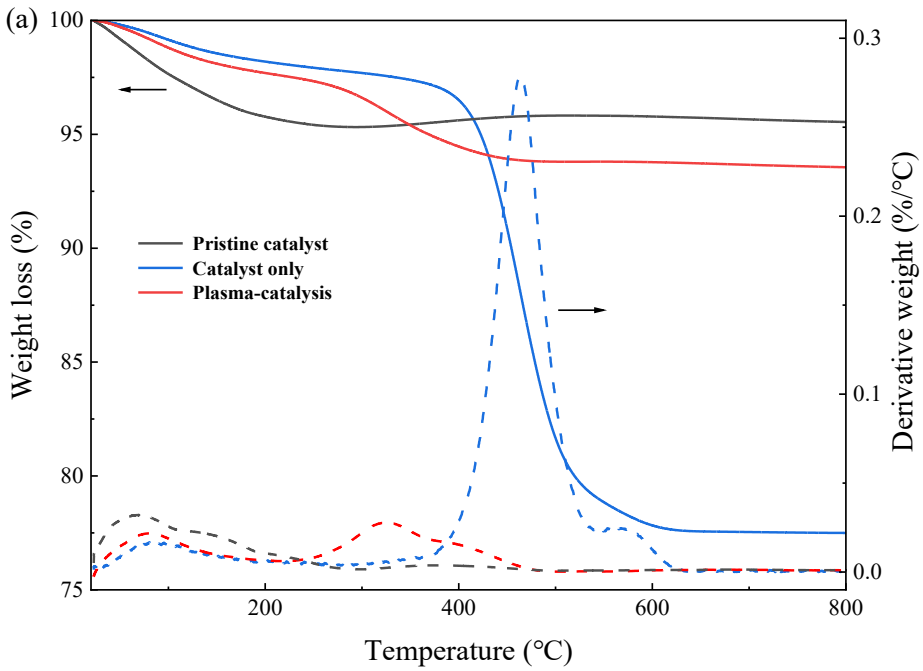

675

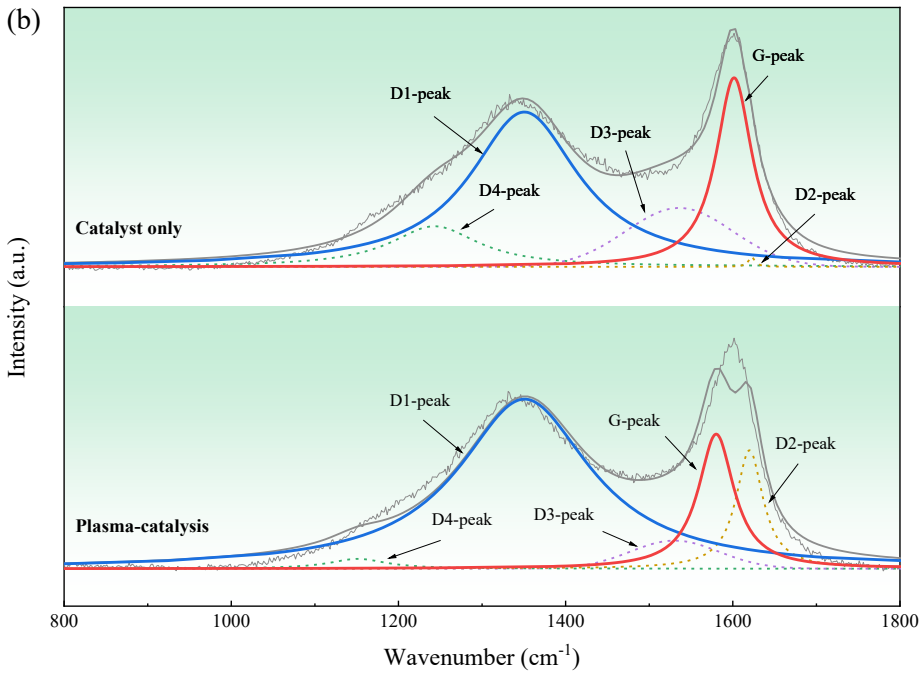

Fig. 10 (a) Temperature programmed oxidation and (b) Raman spectra of spent catalysts after stability test under catalyst only reforming and plasma-catalysis reforming.

Temperature programmed oxidation (TPO) was carried out to identify the carbon deposit on the spent catalysts under catalyst only and plasma-catalysis reforming, depicted as Fig. 10a. As can be observed, there are two marked peaks in each derivative weight loss curves of used catalyst. Thereby, the TPO process can be basically divided into two principal stages: (i) weight loss in the range of 100-250℃ representing the removal of moisture and (ii) weight loss in the range of 250-700℃ representing the combustion of coke deposition. The weight loss at first and then slight increase of pristine catalyst curves can be attributed to the water evaporation and the partial oxidation of active metals Ni, Fe and Ni-Fe alloy, consistent with XRD results in Fig. 11a, which is similar to previous report[61]. Clearly, the coke removal peak is dominating one in each curve, where the carbon deposited on spent catalyst during plasma-catalysis reforming process was significantly less than that without plasma. The Ni-Fe bimetallic catalyst was not considered having strong ability in restraining the coke forming due to no promoter addition like Ce. Therefore, less coke deposition on

693 catalyst under plasma-catalysis mode can be ascribed to the enhancement of Water-gas
694 reaction (R8), Boudouard reaction (R9) and possible cracking of heavy tar adhered,
695 triggering by plasma discharge, which is in line with deduction reported elsewhere[49,
696 62]. Although there still exists coke formation after long-term operation, the
697 regeneration and maintenance costs can be effectively reduced for this integrated
698 system during commercialization. These findings exhibit the ability to coke deposition
699 resistance of catalyst can be upgraded with plasma-catalysis system.

700 Also, the lower oxidation temperature of plasma-catalysis condition demonstrates
701 that the depositing coke might be richer in amorphous carbon, compared to that of
702 catalyst only mode with more filamentous/graphitic carbon. Because according to
703 literature, the amorphous carbon can be oxidized at lower temperature than the latter[63,
704 64]. Raman spectroscopy was applied to further probe into the carbon species in spent
705 catalysts, where the peak fitting was also conducted based on Sheng's method[65].
706 According to Fig. 10b, it can be found that, in both curves (catalyst only and plasma-
707 catalysis), two main peaks located at 1350 cm^{-1} (D1-peak) and 1580 cm^{-1} (G-peak)
708 correspond to amorphous carbon species and filamentous/graphitic carbon species,
709 respectively. The peak intensity ratio of I_G/I_{D1} can be calculated as an indicator to
710 express the coke structure and order degree[66]. The I_G to I_{D1} ratio decreased from 1.22
711 to 0.79 after introduction of plasma assistance, indicating that the more amorphous
712 carbon deposition was produced under plasma-catalysis system rather than graphitic
713 coke. Besides, D2 band at 1620 cm^{-1} can be usually observed together with D1 band
714 according to previous study, where the higher D2-peak intensity of plasma-catalysis
715 sample also shows its inferior degree of carbon structure order[67]. These results
716 basically agree with TPO analysis. More highly disordered amorphous carbon species,
717 known as structural defects, in spent catalyst under plasma-catalysis system can not

only serve as active sites for reforming reaction but make it easy to remove and regenerate.

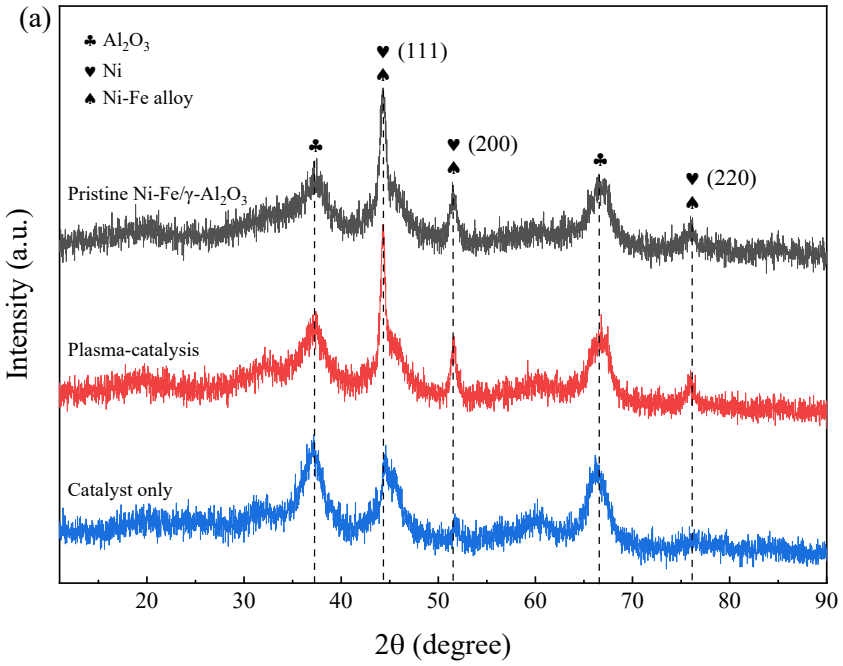

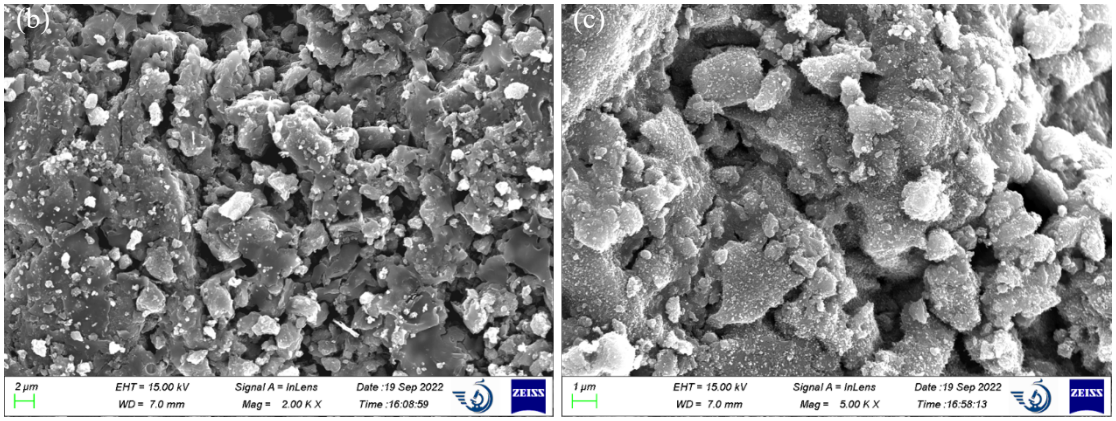

Fig. 11 (a) XRD patterns and (b) (c) SEM images of spent catalysts after stability test under catalyst only reforming and plasma-catalysis reforming.

After stability test under catalytic reforming processes with and without plasma assistance, the crystal structures of spent catalysts were compared and analyzed by using XRD, plotted as Fig. 11a. From XRD patterns, the main diffraction peaks of spent catalysts can be found at identical location of pristine catalysts as discussed above in section 3.1, demonstrating no clear alternation in metal phases and crystal structure. In

729 comparison of pristine and spent catalysts under catalyst only and plasma-catalysis
730 condition, still strong peak intensity of plasma-catalysis mode illustrates a better
731 crystallinity degree than that of spent catalysts without plasma condition, which
732 exhibited a significantly reduced peak intensity. Broadening of diffraction peak can be
733 used to estimate the crystalline average particle size, based on Scherrer equation. As
734 can be seen, the particle size of Ni and Fe detected on the spent catalyst without plasma
735 was larger than that with plasma-catalysis and fresh catalyst. These phenomena can be
736 interpreted by more severe coke deposition and metals sintering when using catalyst for
737 long-term reforming process. The results also well agree with the TPO and SEM
738 analysis. Whereas, with plasma enhancement, the system showed better ability for
739 protection of catalyst from crystallites change and active phase sintering, bring about
740 superior performance during stability tests for H_2 production.

741 To probe into the effects of long-time reaction on surface morphology, SEM was
742 adopted to determine the spent catalysts. Fig. 11b and c displays the SEM images of
743 used catalyst with and without plasma involved reforming process, respectively.
744 Compared with the fresh catalyst morphology shown as Fig. S1(a), the spent catalyst
745 after catalyst only mode tended to be rough and loose, with apparent coral-like
746 substances existing and larger metal particles blocking pores. It is because the formation
747 of marked graphitic coke and carbon nanotubes, as well as aggregation of metallic phase
748 due to sintering after 10 reaction cycles. In contrast, morphology of spent catalyst after
749 stability test with plasma participation still presented relatively sufficient porosity and
750 smooth texture. Not distinct accumulation and coverage of carbon deposition can also
751 be observed, which is in keeping with previous results of performance and
752 characterization.

753

Table 1 Textual properties of pristine catalyst and spent catalysts after stability test under catalyst only reforming and plasma-catalysis reforming.

Sample	BET surface area (m^2/g)	Total pore volume (cm^3/g)	Average pore diameter (nm)
Pristine catalyst	117.60	0.30	10.30
Catalyst only	49.17	0.13	10.67
Plasma-catalysis	82.33	0.24	10.69

As shown in Fig. S6, N_2 adsorption-desorption isotherms and pore size distributions were employed to characterize the structure features of fresh and spent catalyst with and without plasma environment during stability tests, of which the detailed textual properties of different samples are listed in Table 1. According to Fig. S6, both isotherms of spent catalysts were assigned to type IV isotherm shape with H2 type hysteresis loop, on account of the mesoporous feature of γ-Al_2O_3 supporter. N_2 adsorption-desorption isotherms also confirm that the spent catalyst under plasma discharge can be protected from porosity structure blockage and impairment. From BET results shown in Table 1, the BET surface area, total pore volume and average pore diameter of pristine bimetallic catalyst was 117.60 m^2/g, 0.30 cm^3/g and 10.30 nm, respectively. After stability experiments, the spent catalyst without plasma action shows significant reduction in BET surface area and total pore volume, which can be deduced as the consequences from the pores blockage by coke deposited and sintering of metal particles. By comparison, acceptable BET surface area and total pore volume results can be still attained for the used catalyst in plasma-catalysis system. This also well agrees with the previous SEM and XRD results, and ensures a fair performance of H_2 production, because higher specific surface area and porosity can facilitate the

contact between catalyst and reactants to enhance catalytic effects of reaction. Besides, the similar average pore diameters illustrate that the basic physical structure of catalyst cannot be changed by either long-term reaction or plasma discharge. In general, on basis of above characterizations, the protection effect of plasma-catalysis system on catalyst from rapid deactivation during catalytic reforming stage can be well observed and proved.

3.4 Proposed synergistic mechanism of plasma-catalysis system for biomass volatiles

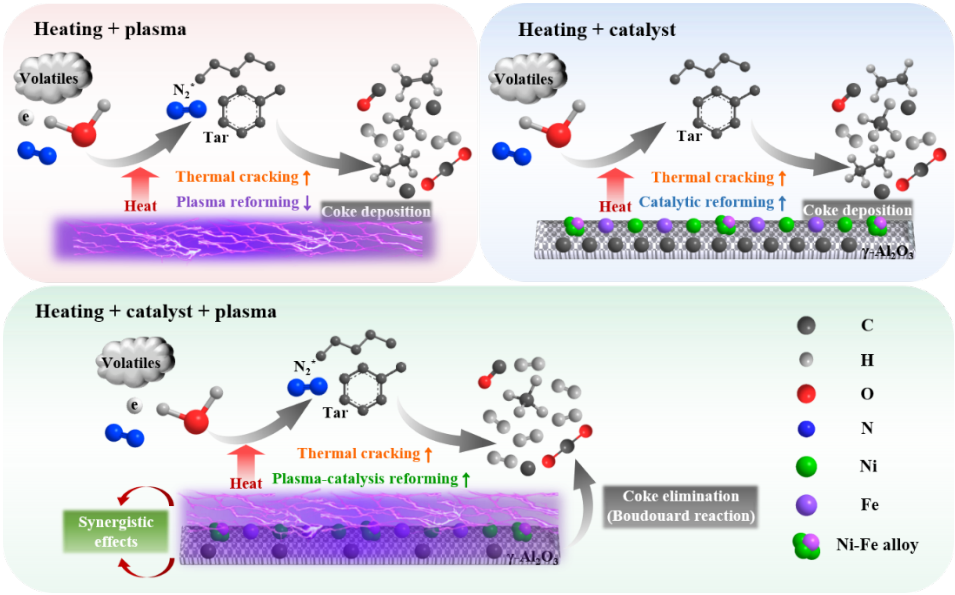

Fig. 12 Proposed synergistic mechanism of plasma-catalysis system for biomass volatiles.

To illustrate roles of temperature and catalyst in this novel integrated pyrolysis and plasma-catalysis system, the proposed synergistic mechanism of plasma-catalysis mode during H_2 production from biomass volatiles is depicted as Fig. 12, compared with plasma-only mode and catalyst-only mode. After the volatiles derived from biomass pyrolysis in upper stage enter the lower reforming stage, plasma reforming can help to gases production, but is inhibited by heating up due to impairment to plasma characteristics. In conventional catalytic reforming, temperature elevation can accelerate reaction rates under catalyst promotion. While, severe coke deposition and

791 metals sintering may occur after long-term operation, leading to the reaction
792 termination. As for plasma-catalysis system, plasma can collaborate with bimetallic
793 catalyst involved to optimize the H_2 production and gaseous products distribution by
794 their synergy effects. For one thing, highly energetic electrons and active species
795 generated in discharge zone facilitate the dissociation and cracking of heavy
796 hydrocarbon and tars, which allows acceleration of reactions at relatively low
797 temperature and assists entrance of reactants into porous structure of catalyst for
798 performance improvement. For another, with plasma assistance, the system also
799 outperforms others in terms of tar elimination and coke resistance through decomposing
800 heavy hydrocarbons and carbon deposit, which significantly extends the lifetime and
801 reduces the maintenance cost of system. Furthermore, synergistic effects are also
802 embodied in the promoted plasma filamentous microdischarges and surface discharges
803 with presence of catalyst, which, in turn, leads to the formation of defects on catalyst,
804 eventually enhancing overall system performance.

805 **4. Conclusions**

806 In this study, as an emerging point of focus, plasma-catalysis was adopted to address
807 major challenges of biomass utilization confronted, through a newly developed
808 integrated pyrolysis and plasma-catalysis system. Roles of temperature and catalyst
809 were tried to understand by investigating different influence factors and discovering
810 synergistic effects between plasma and catalyst during reactions. First, the results show
811 that proper input of discharge power and steam in 2nd reforming stage can boost H_2
812 production from biomass volatiles, thanks to promoted generation of energetic electrons
813 and introduction of H and OH radicals, respectively. Heat supply is recognized as two
814 different influences on plasma-only and plasma-catalysis systems. With only plasma
815 reforming, reaction temperature elevation acts as inhibitor to plasma characters and its

contribution to performance, thus, ambient condition without external heat is recommended for H_2 and syngas production. When packing bimetallic Ni-Fe/γ-Al_2O_3 catalyst into plasma zone, optimal 47.65 mmol/g and 70.53 mmol/g of H_2 and total gas production respectively was attained at reforming temperature of 500℃, where the synergy effects can be observed. Plasma-catalysis system also outperformed in tar cracking, tar elimination and stability test, which can be confirmed and attributed to plasma assistance. This work provides an alternative and evaluation to construct new integrated pyrolysis and plasma-catalysis process for H_2 production from biomass volatiles, Also, its promising commercialization prospects can be highlighted by possibility to couple plasma technology with existing biomass conversion industry for optimized energy production with real biomass resources.

Acknowledgements

The authors would like to appreciate the National Natural Science Foundation of China (No. 52276211), Science and Technology Exchange Project of China Ministry of Science and Technology (No.2021-12-2), Education Cooperation Project between China and Central Eastern European Countries from China Education Association for International Exchange (No. 2021086). We also thank the support of the Instrument Analysis Center of Xi'an Jiaotong University.

References

[1] P. Sharma, B. Gupta, M. Pandey, K. Singh Bisen, P. Baredar, Downdraft biomass gasification: A review on concepts, designs analysis, modelling and recent advances, Materials Today: Proceedings 46 (2021) 5333-5341. https://doi.org/10.1016/j.matpr.2020.08.789.

[2] M.Z. Jacobson, Review of solutions to global warming, air pollution, and energy security, Energy & Environmental Science 2 (2008) 148-173. https://doi.org/10.1039/B809990C.

[3] E.T. Sayed, T. Wilberforce, K. Elsaid, M.K.H. Rabaia, M.A. Abdelkareem, K.J. Chae, A.G. Olabi, A critical review on environmental impacts of renewable energy systems and mitigation strategies: Wind, hydro, biomass and geothermal, Sci Total Environ 766 (2021) 144505.

https://doi.org/10.1016/j.scitotenv.2020.144505.
[4] S. Heidenreich, P.U. Foscolo, New concepts in biomass gasification, Progress in Energy and Combustion Science 46 (2015) 72-95. https://doi.org/10.1016/j.pecs.2014.06.002.
[5] A. Sharma, V. Pareek, D. Zhang, Biomass pyrolysis—A review of modelling, process parameters and catalytic studies, Renewable and Sustainable Energy Reviews 50 (2015) 1081-1096. https://doi.org/10.1016/j.rser.2015.04.193.
[6] M. Sharifzadeh, M. Sadeqzadeh, M. Guo, T.N. Borhani, N.V.S.N. Murthy Konda, M.C. Garcia, L. Wang, J. Hallett, N. Shah, The multi-scale challenges of biomass fast pyrolysis and bio-oil upgrading: Review of the state of art and future research directions, Progress in Energy and Combustion Science 71 (2019) 1-80. https://doi.org/10.1016/j.pecs.2018.10.006.
[7] A. Williams, J.M. Jones, L. Ma, M. Pourkashanian, Pollutants from the combustion of solid biomass fuels, Progress in Energy and Combustion Science 38(2) (2012) 113-137. https://doi.org/10.1016/j.pecs.2011.10.001.
[8] B. Pandey, Y.K. Prajapati, P.N. Sheth, Recent progress in thermochemical techniques to produce hydrogen gas from biomass: A state of the art review, International Journal of Hydrogen Energy 44(47) (2019) 25384-25415. https://doi.org/10.1016/j.ijhydene.2019.08.031.
[9] J. Yang, Q. He, L. Yang, A review on hydrothermal co-liquefaction of biomass, Applied Energy 250 (2019) 926-945. https://doi.org/10.1016/j.apenergy.2019.05.033.
[10] A. Jain, R. Balasubramanian, M.P. Srinivasan, Hydrothermal conversion of biomass waste to activated carbon with high porosity: A review, Chemical Engineering Journal 283 (2016) 789-805. https://doi.org/10.1016/j.cej.2015.08.014.
[11] D. Cheng, H.H. Ngo, W. Guo, S.W. Chang, D.D. Nguyen, L. Deng, Z. Chen, Y. Ye, X.T. Bui, N.B. Hoang, Advanced strategies for enhancing dark fermentative biohydrogen production from biowaste towards sustainable environment, Bioresour Technol 351 (2022) 127045. https://doi.org/10.1016/j.biortech.2022.127045.
[12] A. Kumar, P. Daw, D. Milstein, Homogeneous Catalysis for Sustainable Energy: Hydrogen and Methanol Economies, Fuels from Biomass, and Related Topics, Chem Rev 122(1) (2022) 385-441. https://doi.org/10.1021/acs.chemrev.1c00412.
[13] S. Sharma, S.K. Ghoshal, Hydrogen the future transportation fuel: From production to applications, Renewable and Sustainable Energy Reviews 43 (2015) 1151-1158. https://doi.org/10.1016/j.rser.2014.11.093.
[14] H. Zhang, L. Wang, J. Van herle, F. Maréchal, U. Desideri, Techno-economic comparison of green ammonia production processes, Applied Energy 259 (2020). https://doi.org/10.1016/j.apenergy.2019.114135.
[15] J. Kang, S. He, W. Zhou, Z. Shen, Y. Li, M. Chen, Q. Zhang, Y. Wang, Single-pass transformation of syngas into ethanol with high selectivity by triple tandem catalysis, Nat Commun 11(1) (2020) 827. https://doi.org/10.1038/s41467-020-14672-8.

[16] Y. Wang, M. Craven, X. Yu, J. Ding, P. Bryant, J. Huang, X. Tu, Plasma-Enhanced Catalytic Synthesis of Ammonia over a Ni/Al_2O_3 Catalyst at Near-Room Temperature: Insights into the Importance of the Catalyst Surface on the Reaction Mechanism, ACS Catal 9(12) (2019) 10780-10793. https://doi.org/10.1021/acscatal.9b02538.

[17] I. Ro, Y. Liu, M.R. Ball, D.H.K. Jackson, J.P. Chada, C. Sener, T.F. Kuech, R.J. Madon, G.W. Huber, J.A. Dumesic, Role of the $Cu\text{-}ZrO_2$ Interfacial Sites for Conversion of Ethanol to Ethyl Acetate and Synthesis of Methanol from CO_2 and H_2, ACS Catalysis 6(10) (2016) 7040-7050. https://doi.org/10.1021/acscatal.6b01805.

[18] X. Huang, J. Ren, J.-Y. Ran, C.-L. Qin, Z.-Q. Yang, J.-P. Cao, Recent advances in pyrolysis of cellulose to value-added chemicals, Fuel Processing Technology 229 (2022). https://doi.org/10.1016/j.fuproc.2022.107175.

[19] Z. Yao, S. You, T. Ge, C.-H. Wang, Biomass gasification for syngas and biochar co-production: Energy application and economic evaluation, Applied Energy 209 (2018) 43-55. https://doi.org/10.1016/j.apenergy.2017.10.077.

[20] G. Ravenni, Z. Sárossy, S. Sanna, J. Ahrenfeldt, U.B. Henriksen, Residual gasification char applied to tar reforming in a pilot-scale gasifier: Performance and evolution of char properties for perspective cascade uses, Fuel Processing Technology 210 (2020). https://doi.org/10.1016/j.fuproc.2020.106546.

[21] J. Li, J. Tao, B. Yan, K. Cheng, G. Chen, J. Hu, Microwave reforming with char-supported Nickel-Cerium catalysts: A potential approach for thorough conversion of biomass tar model compound, Applied Energy 261 (2020). https://doi.org/10.1016/j.apenergy.2019.114375.

[22] J. Mazumder, H.I. de Lasa, Catalytic steam gasification of biomass surrogates: Thermodynamics and effect of operating conditions, Chemical Engineering Journal 293 (2016) 232-242. https://doi.org/10.1016/j.cej.2016.02.034.

[23] D.K. Binte Mohamed, A. Veksha, T.-T. Lim, G. Lisak, Hydrogen bromide in syngas: Effects on tar reforming, water gas-shift activities and sintering of Ni-based catalysts, Applied Catalysis B: Environmental 280 (2021). https://doi.org/10.1016/j.apcatb.2020.119435.

[24] D. Yao, Q. Hu, D. Wang, H. Yang, C. Wu, X. Wang, H. Chen, Hydrogen production from biomass gasification using biochar as a catalyst/support, Bioresour Technol 216 (2016) 159-64. https://doi.org/10.1016/j.biortech.2016.05.011.

[25] J. Ashok, S. Kawi, Nickel–Iron Alloy Supported over Iron–Alumina Catalysts for Steam Reforming of Biomass Tar Model Compound, ACS Catalysis 4(1) (2013) 289-301. https://doi.org/10.1021/cs400621p.

[26] N. Gao, J. Salisu, C. Quan, P. Williams, Modified nickel-based catalysts for improved steam reforming of biomass tar: A critical review, Renewable and Sustainable Energy Reviews 145 (2021) 111023. https://doi.org/10.1016/j.rser.2021.111023.

[27] A. George, B. Shen, M. Craven, Y. Wang, D. Kang, C. Wu, X. Tu, A Review of Non-

Thermal Plasma Technology: A novel solution for CO_2 conversion and utilization, Renewable and Sustainable Energy Reviews 135 (2021) 109702. https://doi.org/10.1016/j.rser.2020.109702.

[28] E.C. Neyts, K.K. Ostrikov, M.K. Sunkara, A. Bogaerts, Plasma Catalysis: Synergistic Effects at the Nanoscale, Chemical Reviews 115(24) (2015) 13408-13446. https://doi.org/10.1021/acs.chemrev.5b00362.

[29] H. Chen, Y. Mu, S. Xu, S. Xu, C. Hardacre, X. Fan, Recent advances in non-thermal plasma (NTP) catalysis towards C1 chemistry, Chinese Journal of Chemical Engineering 28(8) (2020) 2010-2021. https://doi.org/10.1016/j.cjche.2020.05.027.

[30] M. Asghari, B. Hosseinzadeh Samani, R. Ebrahimi, Review on non-thermal plasma technology for biodiesel production: Mechanisms, reactors configuration, hybrid reactors, Energy Conversion and Management 258 (2022). https://doi.org/10.1016/j.enconman.2022.115514.

[31] D. Mei, X. Zhu, C. Wu, B. Ashford, P.T. Williams, X. Tu, Plasma-photocatalytic conversion of CO_2 at low temperatures: Understanding the synergistic effect of plasma-catalysis, Applied Catalysis B: Environmental 182 (2016) 525-532. https://doi.org/10.1016/j.apcatb.2015.09.052.

[32] L. Liu, Z. Zhang, S. Das, S. Xi, S. Kawi, $LaNiO_3$ as a precursor of Ni/La_2O_3 for reverse water-gas shift in DBD plasma: Effect of calcination temperature, Energy Conversion and Management 206 (2020). https://doi.org/10.1016/j.enconman.2020.112475.

[33] D. Li, V. Rohani, F. Fabry, A. Parakkulam Ramaswamy, M. Sennour, L. Fulcheri, Direct conversion of CO_2 and CH_4 into liquid chemicals by plasma-catalysis, Applied Catalysis B: Environmental 261 (2020). https://doi.org/10.1016/j.apcatb.2019.118228.

[34] Y. Liu, J. Song, X. Diao, L. Liu, Y. Sun, Removal of tar derived from biomass gasification via synergy of non-thermal plasma and catalysis, Sci Total Environ 721 (2020) 137671. https://doi.org/10.1016/j.scitotenv.2020.137671.

[35] G. Chen, X. Tu, G. Homm, A. Weidenkaff, Plasma pyrolysis for a sustainable hydrogen economy, Nature Reviews Materials 7(5) (2022) 333-334. https://doi.org/10.1038/s41578-022-00439-8.

[36] L. Liu, Q. Wang, J. Song, X. Yang, Y. Sun, Dry reforming of model biomass pyrolysis products to syngas by dielectric barrier discharge plasma, International Journal of Hydrogen Energy 43(22) (2018) 10281-10293. https://doi.org/10.1016/j.ijhydene.2018.04.112.

[37] A. Bogaerts, X. Tu, J.C. Whitehead, G. Centi, L. Lefferts, O. Guaitella, F. Azzolina-Jury, H.-H. Kim, A.B. Murphy, W.F. Schneider, T. Nozaki, J.C. Hicks, A. Rousseau, F. Thevenet, A. Khacef, M. Carreon, The 2020 plasma catalysis roadmap, Journal of Physics D: Applied Physics 53(44) (2020). https://doi.org/10.1088/1361-6463/ab9048.

[38] H. Zhang, X. Li, F. Zhu, K. Cen, C. Du, X. Tu, Plasma assisted dry reforming of methanol

for clean syngas production and high-efficiency CO_2 conversion, Chemical Engineering Journal 310 (2017) 114-119. https://doi.org/10.1016/j.cej.2016.10.104.
[39] Y. Wang, H. Yang, X. Tu, Plasma reforming of naphthalene as a tar model compound of biomass gasification, Energy Conversion and Management 187 (2019) 593-604. https://doi.org/10.1016/j.enconman.2019.02.075.
[40] R. Xu, X. Kong, H. Zhang, P.M. Ruya, X. Li, Destruction of gasification tar over Ni catalysts in a modified rotating gliding arc plasma reactor: Effect of catalyst position and nickel loading, Fuel 289 (2021). https://doi.org/10.1016/j.fuel.2020.119742.
[41] S. Kwon, S.-k. Im, Feasibility of non-thermal plasma gasification for a waste-to-energy power plant, Energy Conversion and Management 251 (2022). https://doi.org/10.1016/j.enconman.2021.114978.
[42] A.H. Khoja, M. Tahir, N.A.S. Amin, Recent developments in non-thermal catalytic DBD plasma reactor for dry reforming of methane, Energy Conversion and Management 183 (2019) 529-560. https://doi.org/10.1016/j.enconman.2018.12.112.
[43] D. Mei, Y. Wang, S. Liu, M. Alliati, H. Yang, X. Tu, Plasma reforming of biomass gasification tars using mixed naphthalene and toluene as model compounds, Energy Conversion and Management 195 (2019) 409-419. https://doi.org/10.1016/j.enconman.2019.05.002.
[44] K. Ray, S. Sengupta, G. Deo, Reforming and cracking of CH_4 over Al_2O_3 supported Ni, Ni-Fe and Ni-Co catalysts, Fuel Processing Technology 156 (2017) 195-203. https://doi.org/10.1016/j.fuproc.2016.11.003.
[45] P.W.C. Groen, A.J. Wolf, T.W.H. Righart, M.C.M.v.d. Sanden, F.J.J. Peeters, W.A. Bongers, Numerical model for the determination of the reduced electric field in a CO_2 microwave plasma derived by the principle of impedance matching, Plasma Sources Science and Technology 28(7) (2019). https://doi.org/10.1088/1361-6595/ab1ca1.
[46] P. Chawdhury, Y. Wang, D. Ray, S. Mathieu, N. Wang, J. Harding, F. Bin, X. Tu, C. Subrahmanyam, A promising plasma-catalytic approach towards single-step methane conversion to oxygenates at room temperature, Applied Catalysis B: Environmental 284 (2021). https://doi.org/10.1016/j.apcatb.2020.119735.
[47] Y.X. Zeng, L. Wang, C.F. Wu, J.Q. Wang, B.X. Shen, X. Tu, Low temperature reforming of biogas over K-, Mg- and Ce-promoted Ni/Al_2O_3 catalysts for the production of hydrogen rich syngas: Understanding the plasma-catalytic synergy, Applied Catalysis B: Environmental 224 (2018) 469-478. https://doi.org/10.1016/j.apcatb.2017.10.017.
[48] C. Wu, Z. Wang, J. Huang, P.T. Williams, Pyrolysis/gasification of cellulose, hemicellulose and lignin for hydrogen production in the presence of various nickel-based catalysts, Fuel 106 (2013) 697-706. https://doi.org/10.1016/j.fuel.2012.10.064.
[49] E. Blanquet, M.A. Nahil, P.T. Williams, Enhanced hydrogen-rich gas production from waste biomass using pyrolysis with non-thermal plasma-catalysis, Catalysis Today 337 (2019)

991 216-224. https://doi.org/10.1016/j.cattod.2019.02.033.
992 [50] H. Xiao, J. Harding, S. Lei, W. Chen, S. Xia, N. Cai, X. Chen, J. Hu, Y. Chen, X. Wang,
993 X. Tu, H. Yang, H. Chen, Hydrogen and aromatics recovery through plasma-catalytic pyrolysis
994 of waste polypropylene, Journal of Cleaner Production 350 (2022).
995 https://doi.org/10.1016/j.jclepro.2022.131467.
996 [51] B. Jiang, S. Zhao, Y. Wang, Y. Wenren, Z. Zhu, J. Harding, X. Zhang, X. Tu, X. Zhang,
997 Plasma-enhanced low temperature NH_3-SCR of NOx over a Cu-Mn/SAPO-34 catalyst under
998 oxygen-rich conditions, Applied Catalysis B: Environmental 286 (2021).
999 https://doi.org/10.1016/j.apcatb.2021.119886.
1000 [52] D.B. Nguyen, Q.H. Trinh, M.M. Hossain, W.G. Lee, Y.S. Mok, Enhancement of plasma-
1001 assisted catalytic CO_2 reforming of CH_4 to syngas by avoiding outside air discharges from
1002 ground electrode, International Journal of Hydrogen Energy 45(36) (2020) 18519-18532.
1003 https://doi.org/10.1016/j.ijhydene.2019.06.167.
1004 [53] C.E. Stere, J.A. Anderson, S. Chansai, J.J. Delgado, A. Goguet, W.G. Graham, C. Hardacre,
1005 S.F.R. Taylor, X. Tu, Z. Wang, H. Yang, Non-Thermal Plasma Activation of Gold-Based
1006 Catalysts for Low-Temperature Water-Gas Shift Catalysis, Angew Chem Int Ed Engl 56(20)
1007 (2017) 5579-5583. https://doi.org/10.1002/anie.201612370.
1008 [54] Y. Chai, N. Gao, M. Wang, C. Wu, H_2 production from co-pyrolysis/gasification of waste
1009 plastics and biomass under novel catalyst Ni-CaO-C, Chemical Engineering Journal 382 (2020).
1010 https://doi.org/10.1016/j.cej.2019.122947.
1011 [55] F. Saleem, K. Zhang, A. Harvey, Role of CO_2 in the Conversion of Toluene as a Tar
1012 Surrogate in a Nonthermal Plasma Dielectric Barrier Discharge Reactor, Energy & Fuels 32(4)
1013 (2018) 5164-5170. https://doi.org/10.1021/acs.energyfuels.7b04070.
1014 [56] J.S. M. Hering, S. Grossmann, U. Riechert, Influence of gas temperature on the breakdown
1015 voltage in gas-insulated systems, IEEE Transactions on Dielectrics and Electrical Insulation
1016 24(1) (2017) 401-408.
1017 [57] F. Rodrigues, J. Pascoa, M. Trancossi, Heat generation mechanisms of DBD plasma
1018 actuators, Experimental Thermal and Fluid Science 90 (2018) 55-65.
1019 https://doi.org/10.1016/j.expthermflusci.2017.09.005.
1020 [58] L. Liu, Z. Zhang, S. Das, S. Kawi, Reforming of tar from biomass gasification in a hybrid
1021 catalysis-plasma system: A review, Applied Catalysis B: Environmental 250 (2019) 250-272.
1022 https://doi.org/10.1016/j.apcatb.2019.03.039.
1023 [59] J. Ren, J.-P. Cao, F.-L. Yang, X.-Y. Zhao, W. Tang, X. Cui, Q. Chen, X.-Y. Wei, Layered
1024 uniformly delocalized electronic structure of carbon supported Ni catalyst for catalytic
1025 reforming of toluene and biomass tar, Energy Conversion and Management 183 (2019) 182-
1026 192. https://doi.org/10.1016/j.enconman.2018.12.093.
1027 [60] X. Tu, J.C. Whitehead, Plasma-catalytic dry reforming of methane in an atmospheric

dielectric barrier discharge: Understanding the synergistic effect at low temperature, Applied Catalysis B: Environmental 125 (2012) 439-448. https://doi.org/10.1016/j.apcatb.2012.06.006.
[61] N. Gao, Y. Han, C. Quan, Study on steam reforming of coal tar over Ni Co/ceramic foam catalyst for hydrogen production: Effect of Ni/Co ratio, International Journal of Hydrogen Energy 43(49) (2018) 22170-22186. https://doi.org/10.1016/j.ijhydene.2018.10.119.
[62] S. Kameshima, K. Tamura, Y. Ishibashi, T. Nozaki, Pulsed dry methane reforming in plasma-enhanced catalytic reaction, Catalysis Today 256 (2015) 67-75. https://doi.org/10.1016/j.cattod.2015.05.011.
[63] S. Ramesh, N.J. Venkatesha, Template Free Synthesis of Ni-Perovskite: An Efficient Catalyst for Hydrogen Production by Steam Reforming of Bioglycerol, ACS Sustainable Chemistry & Engineering 5(2) (2017) 1339-1346. https://doi.org/10.1021/acssuschemeng.6b01744.
[64] J.A. Calles, A. Carrero, A.J. Vizcaíno, L. García-Moreno, Hydrogen production by glycerol steam reforming over SBA-15-supported nickel catalysts: Effect of alkaline earth promoters on activity and stability, Catalysis Today 227 (2014) 198-206. https://doi.org/10.1016/j.cattod.2013.11.006.
[65] C. Sheng, Char structure characterised by Raman spectroscopy and its correlations with combustion reactivity, Fuel 86(15) (2007) 2316-2324. https://doi.org/10.1016/j.fuel.2007.01.029.
[66] D. Yao, H. Li, Y. Dai, C.-H. Wang, Impact of temperature on the activity of Fe-Ni catalysts for pyrolysis and decomposition processing of plastic waste, Chemical Engineering Journal 408 (2021). https://doi.org/10.1016/j.cej.2020.127268.
[67] L. Jin, X. Bai, Y. Li, C. Dong, H. Hu, X. Li, In-situ catalytic upgrading of coal pyrolysis tar on carbon-based catalyst in a fixed-bed reactor, Fuel Processing Technology 147 (2016) 41-46. https://doi.org/10.1016/j.fuproc.2015.12.028.